Advance Publication

The Journal of Veterinary Medical Science

Accepted Date: 4 February 2023

J-STAGE Advance Published Date: 17 February 2023

Field: *Toxicology*

Type: *NOTE*

Next-generation effects of fetal and lactational exposure to the neonicotinoid pesticide clothianidin on the immune system and gut microbiota

Midori MURATA[1)], Asuka SHODA[1)], Mako KIMURA[1)], Yukako HARA[1)], Sakura YONOICHI[1)], Yuya ISHIDA[1)], Youhei MANTANI[2)], Toshifumi YOKOYAMA[1)], Eiko MATSUO[3)], Tetsushi HIRANO[4)] and Nobuhiko HOSHI[1)] *

[1)] *Laboratory of Animal Molecular Morphology, Department of Animal Science, Graduate School of Agricultural Science, Kobe University, 1-1 Rokkodai, Nada, Kobe, Hyogo 657-8501, Japan*

[2)] *Laboratory of Histophysiology, Department of Animal Science, Graduate School of Agricultural Science, Kobe University, 1-1 Rokkodai, Nada, Kobe, Hyogo 657-8501, Japan*

[3)] *Laboratory of Microbiology and Immunology, Department of Animal Science, Graduate School of Agricultural Science, Kobe University, 1-1 Rokkodai, Nada, Kobe, Hyogo 657-8501, Japan*

[4)] *Life Science Research Center, University of Toyama, 2630 Sugitani, Toyama 930-0194, Japan*

*Correspondence to: Hoshi N.: nobhoshi@kobe-u.ac.jp

Running head: NEXT-GENERATION IMMUNOTOXICITY OF CLOTHIANIDIN

ABSTRACT

Recently, the effects of exposure to clothianidin (CLO) on the thymus and gut microbiota have become clear, but no report has examined its next-generation impacts. Pregnant C57BL/6N mice were administered a no-observed-adverse-effect-level dose of CLO until weaning. We examined CLO's effects on the gut microbiota and immune organs of dams and their 3- and 10-week-old male offspring. CLO administration led to several alterations of the top 30 bacterial genera in the gut microbiota in dams and 3-week-old mice. Compared to controls, 10-week-old mice had more thymic Hassall's corpuscles, and both dams and 10-week-old mice had fewer macrophages. These results suggest that fetal and lactational CLO exposure may affect the immune system and gut microbiota of the next generation.

KEYWORDS

clothianidin, dysbiosis, fetal and lactational exposure, Hassall's corpuscles, thymus

Pesticides protect crops by eradicating pests and diseases, contributing greatly to the stable supply of food. Neonicotinoid pesticides (NNs), which are still widely used despite restrictions in Europe and elsewhere, are structurally similar to nicotine and exhibit strong agonist effects on insect nicotinic acetylcholine receptors (nAChRs) [49]. They are considered safe and are widely used in Japan and abroad, with low toxicity to humans. However, NNs were found to affect nAChR-mediated neuroexcitatory action in mammals [27]. Reproductive toxicity [22, 28, 48, 58], cognitive/emotional alterations, and developmental neurotoxicity of NNs [17−19, 21, 32, 45, 46, 59] were later reported, in addition to a systematic review [9] of NNs. nAChR is expressed widely in the nervous system and skeletal muscle as well as in immune cells [26] and regulates antigen presentation, cytokine production, and anti-inflammatory responses [38, 60]. Therefore, it is assumed that NNs may disrupt mammalian immune function via nAChR, but there are very few reports on the immunotoxicity of NNs. The intestinal tract is also called the "headquarters of systemic immunity" or the "largest immune organ"

because approximately 70% of immune cells in the human body are concentrated there. Since the gut microbiota influences host immune responses and metabolic mechanisms through complex interactions [47], it has been shown that dysbiosis, an imbalance of the gut microbiota, causes allergies [41], immunomodulatory disorders [39], and neuropsychiatric disorders [25]. Our previous study revealed that subchronic ingestion of clothianidin (CLO), a type of NN, caused a decrease in thymus weight and induced dysbiosis in rats [36], showing for the first time an association between NNs and dysbiosis in mammals. In addition, CLO and its metabolites are rapidly transferred from pregnant dam to fetus [34] and are highly concentrated in breast milk [43]. They are detected in the urine of human newborns and children [23, 24, 37], and the next-generation effects of NN exposure are of concern [28, 32]. However, there have been no reports on the next-generation effects of NNs on the immune system and gut microbiota of mammals. In this study, we examine CLO's next-generation effects on the immune system by analyzing changes in the thymus and in bacterial flora in the cecal contents of mice. Cecal contents are not contaminated by external bacteria until the time of collection, compared to feces that have been discharged from the body. We also used the cecal contents to compare our present results with those of the previous study, which used rat cecal contents for microbiota analysis [36].

Pregnant C57BL/6NCrSlc mice were purchased from Japan SLC (Hamamatsu, Japan) and maintained as described elsewhere [19]. The present study was approved by the Institutional Animal Care and Use Committee (Permission #30-01-01) and conducted in accordance with the Kobe University Animal Experiment Regulations.

We purified CLO with 95% purity according to the method of a previous study [18] and divided dams into two groups: a CLO-0 group (1% dimethyl sulfoxide) and a CLO-65 group (65 mg CLO/kg body weight/day). The administration concentration was set with reference to the no-observed-adverse-effect-level (NOAEL) of 65.1 mg CLO/kg/day [13, 51].

To eliminate the risk of adverse effects associated with gavage, the dams (F0) were given rehydration gel (MediGel® Sucralose; ClearH2O, Portland, ME, USA) with or without CLO from gestational day 1.5 to postnatal day (PND) 21, when the litters (F1) were weaned as described elsewhere [28].

Each litter was randomly culled to a maximum of 6 pups on PND 3 to standardize the amount of milk. No more than 2 offspring from the same dam were used per group.

On PND 21, the dams and male pups were euthanized by whole blood collection from the heart under deep anesthesia with isoflurane, and the thymus, spleen, adrenal gland, and cecal contents were removed from the dams and pups. The thymus, spleen, and adrenal gland were weighed after trimming. The thymi were then fixed in 4% paraformaldehyde in 0.1 M phosphate buffer at 4°C for 6 hr. They were embedded in paraffin according to the established method. Cecal contents were frozen with liquid nitrogen in 1.5 mL Eppendorf tubes and stored in a –80°C freezer until use. Samples were collected from the 10-week-old male mice in the same way. Finally, 4-μm-thick sections were cut by a sliding microtome (SM2000R; Leica Microsystems, Wetzlar, Germany) and mounted on glass slides precoated with 2% 3-aminopropyltriethoxysilane (Shin-Etsu Chemical Co., Tokyo, Japan). Sections were stored at –30°C until use. For the general histological analyses, tissue sections were stained with hematoxylin and eosin after deparaffinization and hydration. In addition, we measured the cortical and medullary areas of the stained images by using ImageJ software (National Institutes of Health, Bethesda, MD, USA). The Hassall's corpuscles observed in the medulla were counted per mm^2. Immunohistochemical analysis using anti-mouse CD68 antibody (1:2,000; ab125212; Abcam, Cambridge, UK), a tissue macrophage marker, was performed according to a previous report [36]. At this time, we retrieved antigens by heating the sections at 121°C for 20 min in 10 mM sodium citrate (pH 6.0).

The CD68-positive areas of the stained images were measured and compared using ImageJ software. The positive areas were determined by extracting the DAB color using the "Color Deconvolution" function and then setting the upper limit for removing the coloration caused by nonspecific reactions using the "Threshold" command. The areas were measured by the "Measure" command, and the CD68-positive area ratios were calculated and compared.

We extracted and purified DNA of the gut microbiota from the cecal contents using a nucleic acid purification system (Maxwell® RSC; Promega K.K., Tokyo, Japan) and a nucleic acid purification kit (Maxwell® RSC Fecal Microbiome DNA Kit [AS 1700]; Promega K.K.) following the manufacturer's

instructions. The analysis of gut microbiota by 16S rRNA sequencing of the collected samples was entrusted to Azenta Japan Corp. (Tokyo, Japan), which performed the analysis as previously described [36]. In short, sequencing was performed using a 2 × 300 paired-end (PE) configuration; image analysis and base calling were conducted by the MiSeq Control Software embedded in the MiSeq instrument. Valid sequences for cluster analysis were obtained from DNA samples, and taxonomic analysis was performed on representative sequences of each cluster. Clusters were formed by 97% sequence identity, and sequences were grouped into operational taxonomic units (OTU) using the clustering program VSEARCH (1.9.6). Based on the results of the OTU analysis, the species richness and uniformity of the samples were evaluated.

Statistical analysis was performed with BellCurve for Excel (Version 3.23; SSRI, Tokyo, Japan). The sex ratio of the pups was analyzed by the Cochran–Mantel–Haenszel test. The number of pups, body weights, organ weights, the numbers of Hassall's corpuscles, and the CD68-positive area ratio of the thymus were analyzed by Welch's *t*-test. Differences in the relative abundance of OTUs and in the α diversity indexes of gut microbiota were analyzed by two-way ANOVA (CLO × age) followed by Bonferroni *post hoc* tests. The results were considered significant when the *P*-value was less than 0.05.

CLO showed no significant effect on the total number of offspring per dam or on the sex ratio. There was no statistically significant difference in the body weight of F1 generation mice between the CLO-0 and CLO-65 groups at either 3 or 10 weeks of age, when we collected samples (Table 1).

The organ weights are shown in Fig. 1. In F0 generation mice, there were no statistically significant differences in thymus weight (P=0.263) (Fig. 1A) or spleen weight (P=0.404) (Fig. 1B). Adrenal gland weight was significantly (P<0.05) lower in the CLO-65 group compared to the CLO-0 group (Fig. 1C). In 3-week-old F1 generation mice, there were no statistically significant differences in thymus weight (P=0.948) (Fig. 1D) or spleen weight (P=0.518) (Fig. 1E). Adrenal gland weight tended to be lower in the CLO-65 group than in the CLO-0 group (P=0.078) (Fig. 1F). In 10-week-old F1 generation mice, there were no statistically significant differences in thymus weight (P=0.854) (Fig. 1G) or adrenal gland weight (P=0.150) (Fig. 1I). Spleen weight tended to be higher in the CLO-65 group than in the CLO-0

group (P=0.093) (Fig. 1H). As mentioned above, adrenal gland weights were decreased in the F0 generation CLO-65 group and in the F1 3-week-old CLO-65 group (Fig. 1C, 1F). The hypothalamic–pituitary–adrenal (HPA) axis has been reported to interact with the immune system, and HPA axis failure may be observed in autoimmune or inflammatory diseases [4]. In our previous study, the corticosterone level was significantly lower in F1 generation (female) mice when CLO was administered in a manner similar to that in the present study [28]. CLO has also been shown to have the potential for high storability in the fetal adrenal gland [unpublished data]. Thus, CLO's effect on the adrenal gland is thought to be significant; CLO exposure may cause a decrease in adrenal gland weight and may also affect the immune system. The F0 generation CLO-65 group and the F1 3-week-old CLO-65 group, both of which showed decreased adrenal gland weight, were exposed to CLO directly via gel, placenta, or breast milk [34, 43]. Therefore, it is possible that CLO's effect was greater in these 2 groups than in the F1 10-week-old CLO-65 group, and the effect was observed as a decrease in adrenal gland weight in both groups. On the other hand, there was no decrease in thymus weight even in the F0 group (Fig. 1A, 1D, 1G). In one of our previous studies [36], subchronic exposure of rats to CLO resulted in a remarkable decrease in thymus weight, but that experiment was conducted by gavage and the concentration of CLO was approximately 10 times the NOAEL. Thus, CLO's effect on thymus weight may be greater than found in the present study. Therefore, although the effects shown in the previous study did not appear in the present one, CLO may have affected the maintenance of normal thymus morphology.

The general histological analyses of thymus by HE staining (Fig. S1) revealed that the corticomedullary border was indistinct in the CLO-65 group compared with the CLO-0 group, especially in the 3-week-old F1 generation (Fig. S1B) and the 10-week-old F1 generation (Fig. S1C), whereas there was no predominant change in the F0 generation (Fig. S1A). Moreover, we found a significant (P<0.05) increase in Hassall's corpuscles in the 10-week-old F1 generation (Fig. 2). Hassall's corpuscles are composed of keratinized thymic epithelial cells under partial control of the transcription factor Aire. They are well developed in humans and guinea pigs but are virtually absent in normal mice and rats [11].

Thus, their increase in the thymus may have been due to CLO exposure. It has been reported that the formation and proliferation of Hassall's corpuscles may be related to adrenocortical hormone and adrenocorticotropic hormone [16]. In addition, their development is remarkably enhanced in mice lacking transforming growth factor beta receptor II (TGFβ RII) expression in thymic epithelial cells [35]. In other words, suppression of the TGFβ signaling pathway may cause an increase in the number of Hassall's corpuscles. This pathway is suppressed in rats exposed to nicotine prenatally [8]. Therefore, it may also have been suppressed in this study, which would explain the remarkable increase in Hassall's corpuscles. TGFβ has also been reported to be involved in the induction of Th17 cells and in immunosuppression. Therefore, CLO exposure may also inhibit the normal function of the immune system by suppressing the TGFβ signaling pathway. In addition, it has been reported that thymic neutrophils and plasmacytoid dendritic cells (pDCs) are in a highly activated state in New Zealand White mice that have hyperplasia of Hassall's corpuscles, and that IFNα secreted from activated dendritic cells promotes the maturation of single positive T cells [54]. Moreover, thymic stromal lymphopoietin secreted by Hassall's corpuscles activates dendritic cells, which differentiate $CD4^+CD8^-CD25^-$ T cells into natural regulatory T cells (nTreg cells) [55]. Although the exact correlation between the development of Hassall's corpuscles and the differentiation of $Foxp3^+$ Treg cells is still unclear, evidence that medullary thymic epithelial cells (mTECs) could generate specific Treg cells has accumulated [2, 53]. Note that the α3-subunit of nAChR was abundantly expressed in terminally differentiated mTECs, forming Hassall's corpuscle-like structures in the murine thymus [44]. The present and previous results together suggest the possibility that CLO or its metabolic products directly or indirectly stimulate thymic-derived cells, including thymocytes and various subsets of mTECs, to disrupt thymocyte differentiation and maturation.

The results of immunohistochemical analyses of the thymus using CD68 as a marker are shown in Fig. 3 and Fig. S2. In the CLO-65 group compared to the CLO-0 group, the CD68-positive area ratios of F0 generation mice showed a decreasing trend in the thymic cortex (P=0.055) (Fig. 3B, S2A), a significant decrease in the thymic medulla (P<0.05) (Fig. 3C, S2A), and a decreasing trend in the whole

thymus (P=0.057) (Fig. 3A, S2A). Although there was no significant difference between the CLO-0 and CLO-65 groups in any site of the thymus in the 3-week-old F1 generation (Fig. 3D–F, S2B), a decreasing trend was observed in the 10-week-old F1 generation medulla in the CLO-65 group compared to the CLO-0 group (P=0.083) (Fig. 3I, S2C). The decrease in the CD68-positive area ratio of the thymus in the F0 generation and in the 10-week-old F1 generation by CLO exposure is consistent with the significant decrease in the CD68-positive area of rat thymus by CLO exposure in a previous study [unpublished data]. Macrophage functions include phagocytosis, antigen presentation, and cytokine production [12, 33, 40, 57]. In the thymus, macrophages contribute to the normal differentiation and maturation of thymocytes by activating T cells and rapidly removing thymocytes that should be eliminated through positive or negative selection. Therefore, the result that CLO's effects decreased the number of macrophages in the thymus may in turn affect the immune system.

We analyzed the gut microbiota of the cecal contents and found no significant difference in the relative abundance of microbiota on the phylum level between the CLO-0 and CLO-65 groups (Fig. 4A). Among the top 30 OTUs in bacterial composition at the genus level, 2 species in the F0 generation CLO-65 group showed significant alterations, and 5 species in the 3-week-old F1 generation CLO-65 groups showed significant trend alterations in relative abundance compared to the control groups (Fig. 4B, Table 2). In the F0 generation CLO-65, *Alistipes* and *Clostridia_UCG-014* were significantly (P<0.05) decreased compared to the CLO-0 group. In the 3-week-old F1 generation CLO-65 group compared to the CLO-0 group, *Roseburia*, *Lactobacillus*, *f__Peptococcaceae_Unclassified*, and *Butyricicoccus* were significantly (P<0.05) increased, whereas *Oscillibacter* was significantly (P<0.05) decreased. Age had a significant main effect on the relative abundance of *Alistipes*, *Roseburia*, and *Oscillibacter* [F(2, 30)=20.7671, P<0.001; F(2, 30)=5.3064, P<0.05; F(2, 30)=7.7779, P<0.01]. Age also had a significant main effect on the relative abundance of *Clostridia_UCG-014* with significant interaction [F(2, 30)=5.4717, P<0.01; F(2, 30)=3.8567, P<0.05]. Age and CLO had significant main effects on the relative abundance of *Lactobacillus* [F(2, 30)=13.3989, P<0.001; F(2, 30)=6.9552, P<0.05]. CLO had a significant main effect on the relative abundance of *f__Peptococcaceae_Unclassified* with a significant

interaction [F(2, 30)=6.6183, P<0.05; F(2, 30)=3.4658, P<0.05]. Age had a significant main effect, and CLO close to a significant main effect, on the relative abundance of *Butyricicoccus* [F(2, 30)=5.5106, P<0.01; F(2, 30)=3.1879, P=0.084]. In the F0 generation mice, the relative abundance of species that correlated inversely with intestinal inflammation (*Alistipes*, *Clostridia_UCG-014*) was reduced. In the 3-week-old F1 generation mice, the relative abundance of species involved in the production of lactic acid or butyric acid (*Roseburia*, *Lactobacillus*, *Butyricicoccus*) was increased. It has been reported that butyrate produced by gut microbiota maintains homeostasis of the intestinal immune system by inducing differentiation into Treg cells and has an anti-inflammatory effect [14]. On the other hand, no alteration at the genus level was observed in the treated 10-week-old F1 generation groups. These results indicate that the results in the 3-week-old groups, indicating a suppressive effect on inflammation, were transient.

We analyzed the α diversity of gut microbiota, a measure of species richness or uniformity in an environment, using four statistical indices: abundance-based coverage estimator (ACE) (Fig. 5), Chao1 (Fig. S3A), Shannon (Fig. S3B), and Simpson (Fig. S3C). Alpha diversity is an important indicator in explaining the diversity of the intestinal microbiota, and some reports suggest an association between α diversity and disease [31]. ACE and Chao1 estimate community richness, Shannon and Simpson estimate community diversity. ACE showed an increasing trend (P=0.081) in the CLO-65 group compared to the CLO-0 group in the F0 generation, and a significant (P<0.05) increase in the CLO-65 group compared to the CLO-0 group in the 10-week-old F1 generation (Fig. 5). There were no statistically significant differences in the remaining three indicators (Fig. S3). Age and CLO had significant main effects [F(2, 29)=95.4874, P<0.001; F(2, 29)=10.0930, P<0.01]. In the relative abundance curve, the 3-week-old F1 generation CLO-0 group showed the shortest abscissa, reflecting the above results (Fig. S4). There were no significant differences in 3 out of 4 indices of α diversity of gut microbiota, and the results of ACE did not indicate a remarkable effect of CLO on diversity, suggesting that CLO's effect on the diversity of gut microbiota was small. Beta diversity, a measure of the degree of similarity between different environments, was calculated using weighted and unweighted UniFrac, and multivariate analyses such as principal coordinate analysis (PCoA) and NMDS analysis

were performed. Visualizing the similarity between the samples by plotting each sample two-dimensionally, we found no significant differences attributable to CLO. However, especially in the F0 generation and the 10-week-old F1 generation, the CLO-65 groups showed less variation in samples within the same group compared to the CLO-0 groups (Fig. S5).

Moreover, analysis of similarities (ANOSIM) showed *R*-values close to 0, so no trend of separation was found between the CLO-0 and CLO-65 groups in the F0 and F1 generation (Table 3). The closer the *R*-value is to 0, the less significant the difference between groups is compared to the difference within groups; the closer it is to 1, the more significant the difference between groups is compared to the difference within groups.

Our previous study [36] significantly differed from the present study in that the former used rats, intragastric administration (gavage), two dose groups (NOAEL and 10 times NOAEL), and male animals that are generally more susceptible to CLO [29]. In addition, previous study showed the variation in the genus of bacteria that produce short-chain fatty acids, which are known to be involved in the induction of Treg cells, macrophages, and dendritic cells [14, 50]. In the present study, no variation was observed at the phylum level, and a significant increase or increasing trend in α diversity was observed in the F0 generation and 10-week-old F1 generation in the CLO-65 group compared to the CLO-0 group. Moreover, as in our previous study, variation of butyrate-producing bacteria was observed in the F0 and F1 generations. In the previous study, no significant variation in the composition of the bacterial flora was observed in the group that received an equal amount of CLO as the NOAEL, whereas significant variation at the phylum level was observed in the group that received a 10 times NOAEL dose. These results suggest that although the effects of an NOAEL dose of CLO on the gut microbiota are not significant, CLO may variate the composition of the gut microbiota of the next generation and may also affect the immune system.

This study revealed that CLO's effect on gut microbiota extends to the next generation. Gut microbiota is reported to be associated with autoimmune diseases such as ulcerative colitis, Crohn's disease, atopic dermatitis, and rheumatoid arthritis as well as depression, a neuropsychiatric disorder

[52]. Therefore, CLO causing dysbiosis of the next generation is a serious problem that may have various adverse effects on the health of the next generation.

CONFLICT OF INTEREST

The authors declare that there are no conflicts of interest.

ACKNOWLEDGMENTS

This work was supported in part by Grants-in-Aid for Scientific Research B (JP22H03750 & JP19H04277: NH), by a Grant-in-Aid for Challenging Exploratory Research (JP21K19846: NH), and by a Grant-in-Aid for Early-Career Scientists (JP19K19406 & 22K17342: TH) from the Japan Society for the Promotion of Science. We also acknowledge financial support from “Act Beyond Trust” (GIA) civil grants in 2020 and 2021 (NH). The funders had no role in the study design, data collection and analysis, decision to publish, or preparation of the manuscript.

REFERENCES

1. Aizawa E, Tsuji H, Asahara T, Takahashi T, Teraishi T, Yoshida S, Ota M, Koga N, Hattori K, Kunugi H. 2016. Possible association of *Bifidobacterium* and *Lactobacillus* in the gut microbiota of patients with major depressive disorder. *J Affect Disord* **202**: 254–257. doi: 10.1016/j.jad.2016.05.038.

2. Aschenbrenner K, D'Cruz LM, Vollmann EH, Hinterberger M, Emmerich J, Swee LK, Rolink A, Klein L. 2007. Selection of Foxp3^{+} regulatory T cells specific for self antigen expressed and presented by Aire^{+} medullary thymic epithelial cells. *Nat Immunol* **8**: 351–358. doi: 10.1038/ni1444.

3. Bankole A, Luo X, Husen Z. 2017. A comparative analysis of gut microbiota between systemic lupus erythematosus patients and non-autoimmune controls: a single center cohort experience. *Lupus Sci Med* **4**. doi: 10.1136/lupus-2017-000215.354.

4. Bellavance MA, Rivest S. 2014. The HPA - Immune axis and the immunomodulatory actions of glucocorticoids in the brain. *Front Immunol* **5**: 136. doi: 10.3389/fimmu.2014.00136.

5. Benno Y. 1991. Identification and classfication of gnus *Lactobacillus*. *Jpn J Food microbiol* **8**: 65 −74. doi: 10.14840/jsfm1984.8.65.

6. Boesmans L, Valles-Colomer M, Wang J, Eeckhaut V, Falony G, Ducatelle R, Van Immerseel F, Raes J, Verbeke K. 2018. Butyrate producers as potential next-generation probiotics: Safety assessment of the administration of *Butyricicoccus pullicaecorum* to healthy volunteers. *mSystems* **3**: e00094-18. doi: 10.1128/mSystems.00094-18.

7. Borton MA, Sabag-Daigle A, Wu J, Solden LM, O'Banion BS, Daly RA, Wolfe RA, Gonzalez JF, Wysocki VH, Ahmer BMM, Wrighton KC. 2017. Chemical and pathogen-induced inflammation disrupt the murine intestinal microbiome. *Microbiom*e **5**: 47. doi: 10.1186/s40168-017-0264-8.

8. Chen B, Lu KH, Ni QB, Li QX, Gao H, Wang H, Chen LB. 2019. Prenatal nicotine exposure increases osteoarthritis susceptibility in male elderly offspring rats via low-function programming of the TGFβ signaling pathway. *Toxicol Lett* **314**: 18–26. doi: 10.1016/j.toxlet.2019.06.010.

9. Costas-Ferreira C, Faro LRF. 2021. Neurotoxic effects of neonicotinoids on mammals: What is there beyond the activation of nicotinic acetylcholine receptors?-A systematic review. *Int J Mol Sci* **22**: 8413. doi: 10.3390/ijms22168413.

10. Duncan SH, Aminov RI, Scott KP, Louis P, Stanton TB, Flint HJ. 2006. Proposal of *Roseburia faecis* sp. nov., *Roseburia hominis* sp. nov. and *Roseburia inulinivorans* sp. nov., based on isolates from human faeces. *Int J Syst Evol Microbiol* **56**: 2437−2441. doi: 10.1099/ijs.0.64098-0.

11. Farr AG, Dooley JL, Erickson M. 2002. Organization of thymic medullary epithelial heterogeneity: implications for mechanisms of epithelial differentiation. *Immunol Rev* **189**: 20 − 27. doi: 10.1034/j.1600-065X.2002.18903.x.

12. Fiorentino DF, Zlotnik A, Mosmann TR, Howard M, O'Garra A. 1991. IL-10 inhibits cytokine production by activated macrophages. *J Immunol* **147**: 3815 − 3822. doi:

10.4049/jimmunol.147.11.3815.

13. Food and Agriculture Organization of the United Nations 2020. FAO Specifications and Evaluations for Agricultural Pesticides Clothianidin. http:// www.fao.org/3/ca7726en/ca7726en.pdf [accessed on November 4, 2020].

14. Furusawa Y, Obata Y, Fukuda S, Endo TA, Nakato G, Takahashi D, Nakanishi Y, Uetake C, Kato K, Kato T, Takahashi M, Fukuda NN, Murakami S, Miyauchi E, Hino S, Atarashi K, Onawa S, Fujimura Y, Lockett T, Clarke JM, Topping DL, Tomita M, Hori S, Ohara O, Morita T, Koseki H, Kikuchi J, Honda K, Hase K, Ohno H. 2013. Commensal microbe-derived butyrate induces the differentiation of colonic regulatory T cells. *Nature* **504**: 446−450. doi: 10.1038/nature12721.

15. Gilmour CC, Podar M, Bullock AL, Graham AM, Brown SD, Somenahally AC, Johs A, Hurt RA Jr, Bailey KL, Elias DA. 2013. Mercury methylation by novel microorganisms from new environments. *Environ Sci Technol* **47**: 11810–11820. doi: 10.1021/es403075t.

16. Hale LP, Markert ML. 2004. Corticosteroids regulate epithelial cell differentiation and Hassall body formation in the human thymus. *J Immunol* **172**: 617–624. doi: 10.4049/jimmunol.172.1.617.

17. Hirano T, Miyata Y, Kubo S, Ohno S, Onaru K, Maeda M, Kitauchi S, Nishi M, Tabuchi Y, Ikenaka Y, Ichise T, Nakayama SMM, Ishizuka M, Arizono K, Takahashi K, Kato K, Mantani Y, Yokoyama T, Hoshi N. 2021. Aging-related changes in the sensitivity of behavioral effects of the neonicotinoid pesticide clothianidin in male mice. *Toxicol Lett* **342**: 95−103. doi: 10.1016/j.toxlet.2021.02.010.

18. Hirano T, Yanai S, Omotehara T, Hashimoto R, Umemura Y, Kubota N, Minami K, Nagahara D, Matsuo E, Aihara Y, Shinohara R, Furuyashiki T, Mantani Y, Yokoyama T, Kitagawa H, Hoshi N. 2015. The combined effect of clothianidin and environmental stress on the behavioral and reproductive function in male mice. *J Vet Med Sci* **77**: 1207−1215. doi: 10.1292/jvms.15-0188.

19. Hirano T, Yanai S, Takada T, Yoneda N, Omotehara T, Kubota N, Minami K, Yamamoto A, Mantani Y, Yokoyama T, Kitagawa H, Hoshi N. 2018. NOAEL-dose of a neonicotinoid pesticide, clothianidin, acutely induce anxiety-related behavior with human-audible vocalizations in male mice in a novel environment. *Toxicol Lett* **282**: 57–63. doi: 10.1016/j.toxlet.2017.10.010.

20. Hofmeister AE, Berger S, Buckel W. 1992. The iron-sulfur-cluster-containing L-serine dehydratase from *Peptostreptococcus asaccharolyticus*. Stereochemistry of the deamination of L-threonine. *Eur J Biochem* **205**: 743–749. doi: 10.1111/j.1432-1033.1992.tb16838.x.

21. Hoshi N. 2021. Adverse effects of pesticides on regional biodiversity and their mechanisms. pp. 235–247. In. Risks and Regulation of New Technologies. (Matsuda T, Wolff J, Yanagawa T, eds), Springer, Singapore.

22. Hoshi N, Hirano T, Omotehara T, Tokumoto J, Umemura Y, Mantani Y, Tanida T, Warita K, Tabuchi Y, Yokoyama T, Kitagawa H. 2014. Insight into the mechanism of reproductive dysfunction caused by neonicotinoid pesticides. *Biol Pharm Bull* **37**: 1439−1443. doi: 10.1248/bpb.b14-00359.

23. Ichikawa G, Kuribayashi R, Ikenaka Y, Ichise T, Nakayama SMM, Ishizuka M, Taira K, Fujioka K,

Sairenchi T, Kobashi G, Bonmatin JM, Yoshihara S. 2019. LC-ESI/MS/MS analysis of neonicotinoids in urine of very low birth weight infants at birth. *PLoS One* **14**: e0219208. doi: 10.1371/journal.pone.0219208.

24. Ikenaka Y, Miyabara Y, Ichise T, Nakayama S, Nimako C, Ishizuka M, Tohyama C. 2019. Exposures of children to neonicotinoids in pine wilt disease control areas. *Environ Toxicol Chem* **38**: 71–79. doi: 10.1002/etc.4316.

25. Jessurun JG, van Harten PN, Egberts TC, Pijl YJ, Wilting I, Tenback DE. 2016. The relation between psychiatric diagnoses and constipation in hospitalized patients: A cross-sectional study. *Psychiatry J* **2016**: 2459693. doi: 10.1155/2016/2459693.

26. Kawashima K, Yoshikawa K, Fujii YX, Moriwaki Y, Misawa H. 2007. Expression and function of genes encoding cholinergic components in murine immune cells. *Life Sci* **80**: 2314−2319. doi: 10.1016/j.lfs.2007.02.036.

27. Kimura-Kuroda J, Komuta Y, Kuroda Y, Hayashi M, Kawano H. 2012. Nicotine-like effects of the neonicotinoid insecticides acetamiprid and imidacloprid on cerebellar neurons from neonatal rats. *PLoS One* **7**: e32432. doi: 10.1371/journal.pone.0032432.

28. Kitauchi S, Maeda M, Hirano T, Ikenaka Y, Nishi M, Shoda A, Murata M, Mantani Y, Yokoyama T, Tabuchi Y, Hoshi N. 2021. Effects of in utero and lactational exposure to the no-observed-adverse-effect level (NOAEL) dose of the neonicotinoid clothianidin on the reproductive organs of female mice. *J Vet Med Sci* **83**: 746–753. doi: 10.1292/jvms.21-0014.

29. Kubo S, Hirano T, Miyata Y, Ohno S, Onaru K, Ikenaka Y, Nakayama SMM, Ishizuka M, Mantani Y, Yokoyama T, Hoshi N. 2022. Sex-specific behavioral effects of acute exposure to the neonicotinoid clothianidin in mice. *Toxicol Appl Pharmacol* **456**: 116283. doi: 10.1016/j.taap.2022.116283.

30. Li M, Wu YQ, Hu YX, Zhao LP, Zhang CH. 2018. Initial gut microbiota structure affects sensitivity to DSS-induced colitis in a mouse model. *Sci China Life Sci* **61**: 762−769. doi: 10.1007/s11427-017-9097-0.

31. Li ZX, Zhou J, Liang H, Ye L, Lan LY, Lu F, Wang Q, Lei T, Yang XP, Cui P, Huang JG. 2022. Differences in alpha diversity of gut microbiota in neurological diseases. *Front Neurosci* **16**: 879318. doi: 10.3389/fnins.2022.879318.

32. Maeda M, Kitauchi S, Hirano T, Ikenaka Y, Nishi M, Shoda A, Murata M, Mantani Y, Tabuchi Y, Yokoyama T, Hoshi N. 2021. Fetal and lactational exposure to the no-observed-adverse-effect level (NOAEL) dose of the neonicotinoid pesticide clothianidin inhibits neurogenesis and induces different behavioral abnormalities at the developmental stages in male mice. *J Vet Med Sci* **83**: 542–548. doi: 10.1292/jvms.20-0721.

33. Martinez FO, Sica A, Mantovani A, Locati M. 2008. Macrophage activation and polarization. *Front Biosci* **13**: 453−461. doi: 10.2741/2692.

34. Ohno S, Ikenaka Y, Onaru K, Kubo S, Sakata N, Hirano T, Mantani Y, Yokoyama T, Takahashi K, Kato K, Arizono K, Ichise T, Nakayama SMM, Ishizuka M, Hoshi N. 2020. Quantitative elucidation of maternal-to-fetal transfer of neonicotinoid pesticide clothianidin and its metabolites in mice. *Toxicol Lett* **322**: 32−38. doi: 10.1016/j.toxlet.2020.01.003.

35. Odaka C, Hauri-Hohl M, Takizawa K, Nishikawa Y, Yano M, Matsumoto M, Boyd R, Holländer GA. 2013. TGF-β type II receptor expression in thymic epithelial cells inhibits the development of Hassall's corpuscles in mice. *Int Immunol* **25**: 633–642. doi: 10.1093/intimm/dxt026.

36. Onaru K, Ohno S, Kubo S, Nakanishi S, Hirano T, Mantani Y, Yokoyama T, Hoshi N. 2020. Immunotoxicity evaluation by subchronic oral administration of clothianidin in Sprague-Dawley rats. *J Vet Med Sci* **82**: 360−372. doi: 10.1292/jvms.19-0689.

37. Oya N, Ito Y, Ebara T, Kato S, Ueyama J, Aoi A, Nomasa K, Sato H, Matsuki T, Sugiura-Ogasawara M, Saitoh S, Kamijima M. 2021. Cumulative exposure assessment of neonicotinoids and an investigation into their intake-related factors in young children in Japan. *Sci Total Environ* **750**: 141630. doi: 10.1016/j.scitotenv.2020.141630.

38. Parrish WR, Rosas-Ballina M, Gallowitsch-Puerta M, Ochani M, Ochani K, Yang LH, Hudson L, Lin X, Patel N, Johnson SM, Chavan S, Goldstein RS, Czura CJ, Miller EJ, Al-Abed Y, Tracey KJ, Pavlov VA. 2008. Modulation of TNF release by choline requires α7 subunit nicotinic acetylcholine receptor-mediated signaling. *Mol Med* **14**: 567–574. doi: 10.2119/2008-00079.Parrish.

39. Round JL, Mazmanian SK. 2009. The gut microbiota shapes intestinal immune responses during health and disease. *Nat Rev Immunol* **9**: 313−323. doi: 10.1038/nri2515.

40. Sallusto F, Lanzavecchia A. 1994. Efficient presentation of soluble antigen by cultured human dendritic cells is maintained by granulocyte/macrophage colony-stimulating factor plus interleukin 4 and downregulated by tumor necrosis factor alpha. *J Exp Med* **179**: 1109−1118. doi: 10.1084/jem.179.4.1109.

41. Sekirov I, Russell SL, Antunes LCM, Finlay BB. 2010. Gut microbiota in health and disease. *Physiol Rev* **90**: 859−904. doi: 10.1152/physrev.00045.2009.

42. Sheng KL, Xu YF, Kong XW, Wang JM, Zha XD, Wang YZ. 2021. Probiotic *Bacillus cereus* alleviates dextran sulfate sodium-induced colitis in mice through improvement of the intestinal barrier function, anti-inflammation, and gut microbiota modulation. *J Agric Food Chem* **69**: 14810–14823. doi: 10.1021/acs.jafc.1c03375.

43. Shoda A, Nishi M, Murata M, Mantani Y, Yokoyama T, Hirano T, Ikenaka Y, Hoshi N. 2023. Quantitative elucidation of the transfer of the neonicotinoid pesticide clothianidin to the breast milk in mice. *Toxicol Lett* **373**: 33–40. doi: 10.1016/j.toxlet.2022.10.006.

44. Soultanova A, Panneck AR, Rafiq A, Kummer W. 2014. Terminally differentiated epithelial cells of the thymic medulla and skin express nicotinic acetylcholine receptor subunit α3. *BioMed Res Int* **2014**: e757502. doi: 10.1155/2014/757502.

45. Takada T, Yoneda N, Hirano T, Onaru K, Mantani Y, Yokoyama T, Kitagawa H, Tabuchi Y, Nimako C, Ishizuka M, Ikenaka Y, Hoshi N. 2020. Combined exposure to dinotefuran and chronic mild stress counteracts the change of the emotional and monoaminergic neuronal activity induced by either exposure singly despite corticosterone elevation in mice. *J Vet Med Sci* **82**: 350–359. doi: 10.1292/jvms.19-0635.

46. Takada T, Yoneda N, Hirano T, Yanai S, Yamamoto A, Mantani Y, Yokoyama T, Kitagawa H, Tabuchi Y, Hoshi N. 2018. Verification of the causal relationship between subchronic exposures to dinotefuran and depression-related phenotype in juvenile mice. *J Vet Med Sci* **80**: 720–724. doi: 10.1292/jvms.18-0022.

47. Tanemoto S, Sujino T, Kanai T. 2017. Intestinal immune response is regulated by gut microbe. *Jpn J Clin Immunol* **40**: 408−415. doi: 10.2177/jsci.40.408.

48. Tokumoto J, Danjo M, Kobayashi Y, Kinoshita K, Omotehara T, Tatsumi A, Hashiguchi M, Sekijima T, Kamisoyama H, Yokoyama T, Kitagawa H, Hoshi N. 2013. Effects of exposure to clothianidin on the reproductive system of male quails. *J Vet Med Sci* **75**: 755−760. doi: 10.1292/jvms.12-0544.

49. Tomizawa M, Casida JE. 2005. Neonicotinoid insecticide toxicology: mechanisms of selective action. *Annu Rev Pharmacol Toxicol* **45**: 247–268. doi: 10.1146/annurev.pharmtox.45.120403.095930.

50. Trompette A, Gollwitzer ES, Yadava K, Sichelstiel AK, Sprenger N, Ngom-Bru C, Blanchard C, Junt T, Nicod LP, Harris NL, Marsland BJ. 2014. Gut microbiota metabolism of dietary fiber influences allergic airway disease and hematopoiesis. *Nat Med* **20**: 159–166. doi: 10.1038/nm.3444.

51. Uneme H, Konobe M, Akayama A, Yokota T, Mizuta K. 2006. Discovery and development of a novel insecticide “clothianidin”. Sumitomo Kagaku 2. pp. 1−14. https://www.sumitomo-chem.co.jp/english/rd/report/files/docs/20060202_h6t.pdf [accessed on November 4, 2020].

52. Vijay A, Valdes AM. 2022. Role of the gut microbiome in chronic diseases: a narrative review. *Eur J Clin Nutr* **76**: 489–501. doi: 10.1038/s41430-021-00991-6.

53. Vobořil M, Brabec T, Dobeš J, Šplíchalová I, Březina J, Čepková A, Dobešová M, Aidarova A, Kubovčiak J, Tsyklauri O, Štěpánek O, Beneš V, Sedláček R, Klein L, Kolář M, Filipp D. 2020. Toll-like receptor signaling in thymic epithelium controls monocyte-derived dendritic cell recruitment and Treg generation. *Nat Commun* **11**: 2361. doi: 10.1038/s41467-020-16081-3.

54. Wang J, Sekai M, Matsui T, Fujii Y, Matsumoto M, Takeuchi O, Minato N, Hamazaki Y. 2019. Hassall’s corpuscles with cellular-senescence features maintain IFNα production through neutrophils and pDC activation in the thymus. *Int Immunol* **31**: 127–139. doi: 10.1093/intimm/dxy073.

55. Watanabe N, Wang YH, Lee HK, Ito T, Wang YH, Cao W, Liu YJ. 2005. Hassall’s corpuscles instruct dendritic cells to induce $CD4^{+}CD25^{+}$ regulatory T cells in human thymus. *Nature* **436**: 1181–1185. doi: 10.1038/nature03886.

56. Wu MN, Li PZ, An YY, Ren J, Yan D, Cui JZ, Li D, Li M, Wang MY, Zhong GS. 2019. Phloretin ameliorates dextran sulfate sodium-induced ulcerative colitis in mice by regulating the gut microbiota. *Pharmacol Res* **150**: 104489. doi: 10.1016/j.phrs.2019.104489.

57. Wynn TA, Barron L. 2010. Macrophages: master regulators of inflammation and fibrosis. *Semin Liver Dis* **30**: 245–257. doi: 10.1055/s-0030-1255354.

58. Yanai S, Hirano T, Omotehara T, Takada T, Yoneda N, Kubota N, Yamamoto A, Mantani Y, Yokoyama T, Kitagawa H, Hoshi N. 2017. Prenatal and early postnatal NOAEL-dose clothianidin exposure leads to a reduction of germ cells in juvenile male mice. *J Vet Med Sci* **79**: 1196−1203. doi: 10.1292/jvms.17-0154.

59. Yoneda N, Takada T, Hirano T, Yanai S, Yamamoto A, Mantani Y, Yokoyama T, Kitagawa H, Tabuchi Y, Hoshi N. 2018. Peripubertal exposure to the neonicotinoid pesticide dinotefuran affects dopaminergic neurons and causes hyperactivity in male mice. *J Vet Med Sci* **80**: 634–637. doi: 10.1292/jvms.18-0014.

60. Zdanowski R, Krzyżowska M, Ujazdowska D, Lewicka A, Lewicki S. 2015. Role of α7 nicotinic receptor in the immune system and intracellular signaling pathways. *Cent Eur J Immunol* **40**: 373−379. doi: 10.5114/ceji.2015.54602.

FIGURE LEGENDS

Fig. 1

Thymus, spleen, and adrenal organ weights of F0 generation mice (A-C) and 3-week-old (D-F) and 10-week-old (G-I) F1 generation mice. A, B: Clothianidin (CLO) had no effect on thymus and spleen weights in F0 generation mice (CLO-0: n=8; CLO-65: n=9). C: Adrenal gland weight was significantly decreased in the CLO-65 group of F0 generation mice (CLO-0: n=8; CLO-65: n=9). D, E: CLO had no effect on thymus and spleen weights in 3-week-old F1 generation mice (CLO-0: n=6; CLO-65: n=10). F: Adrenal gland weight showed an increasing trend in the CLO-65 group of 3-week-old F1 generation mice (CLO-0: n=6; CLO-65: n=10). G, H: CLO had no effect on thymus or adrenal gland weight in 10-week-old F1 generation mice (CLO-0: n=8; CLO-65: n=10). I: Spleen weight showed an increasing trend in the CLO-65 group of 10-week-old F1 generation mice (CLO-0: n=8; CLO-65: n=10). All data represent means + SD of each group, and circles show the values for individual mice. **P*<0.05 vs. the CLO-0 group.

Fig. 2

The number of Hassall's corpuscles (per area of medulla). A significant increase was observed in 10-week-old F1 generation mice. Data represent means + SD of each group, and circles show the values for individual mice (n=6 in each). **P*<0.05 vs. the CLO-0 group.

Fig. 3

Results of immunoquantitative histological analysis of thymus (CD68) in F0 generation mice (A-C), 3-week-old (D-F), and 10-week-old (G-I) F1 generation mice. A-C: The CD68-positive area ratio showed a decreasing trend in the thymic cortex (B), a significant decrease in the medulla (C), and a decreasing trend in the whole thymus (A) in the CLO-65 group compared to the CLO-0 group in F0 generation mice. D-I: CLO did not affect the CD68-positive area ratio in the 3-week-old F1 generation (D-F), but a decreasing trend was observed in the medulla in the CLO-65 group compared to the CLO-0 group in

10-week-old F1 generation mice (I). All data represent means + SD of each group, and circles show the values for individual mice (n=6 in each). *P<0.05 vs. the CLO-0 group.

Fig. 4

Composition of gut microbiota. A: Relative abundance of gut microbiota (group comparisons at the phylum level). No effect due to CLO was observed. B: Relative abundance of gut microbiota (group comparisons at the genus level). Variability was observed in 2 species in the F0 generation mice and in 5 species in 3-week-old F1 generation mice (indicated by red stars). (A, B: n=6 in each).

Fig. 5

Alpha diversity of gut microbiota (assessment by statistical index ACE).

An increasing trend was observed in the CLO-65 group compared to the CLO-0 group in the F0 generation mice, and a significant increase was observed in the CLO-65 group compared to the CLO-0 group in 10-week-old F1 generation mice. Data represent means + SD of each group, and circles show values for individual mice (n=5-6 in each). *P<0.05 vs. the CLO-0 group.

Fig. S1

Representative examples of hematoxylin and eosin (HE) staining of the thymus in the F0 generation mice (A) and in 3-week-old (B) and 10-week-old (C) F1 generation mice. Especially in the F1 mice, the corticomedullary border was indistinct in the CLO-65 group compared to the CLO-0 group.

Fig. S2

Representative examples of immunoquantitative histological analysis of thymus (CD68) in the F0 generation mice (A) and in 3-week-old (B) and 10-week-old (C) F1 generation mice. A: The CD68-positive area ratio showed a decreasing trend in the thymic cortex and a significant decrease in the medulla in the CLO-65 group compared to the CLO-0 group in F0 generation mice. B: CLO did not

affect the CD68-positive area ratio in the 3-week-old F1 generation. C: The CD68-positive area ratio showed a decreasing trend in the medulla in the CLO-65 group compared to the CLO-0 group in 10-week-old F1 generation mice.

Fig. S3

Alpha diversity of gut microbiota (assessment by statistical index Chao1 (A), Shannon (B), Simpson (C)). No effect of CLO was observed on any of the indices (n=5-6 in each).

Fig. S4

Relative abundance curve. The 3-week-old F1 generation CLO-0 group showed the shortest abscissa, suggesting increased diversity due to CLO (n=6 in each).

Fig. S5

Beta diversity of gut microbiota (NMDS analysis). The plots show similarities in the composition of the bacterial flora. There were no significant differences due to CLO exposure. However, especially in the 10-week-old F1 generation mice, there was less variation within the CLO-65 group than within the CLO-0 group (n=6 in each).

Fig. 1

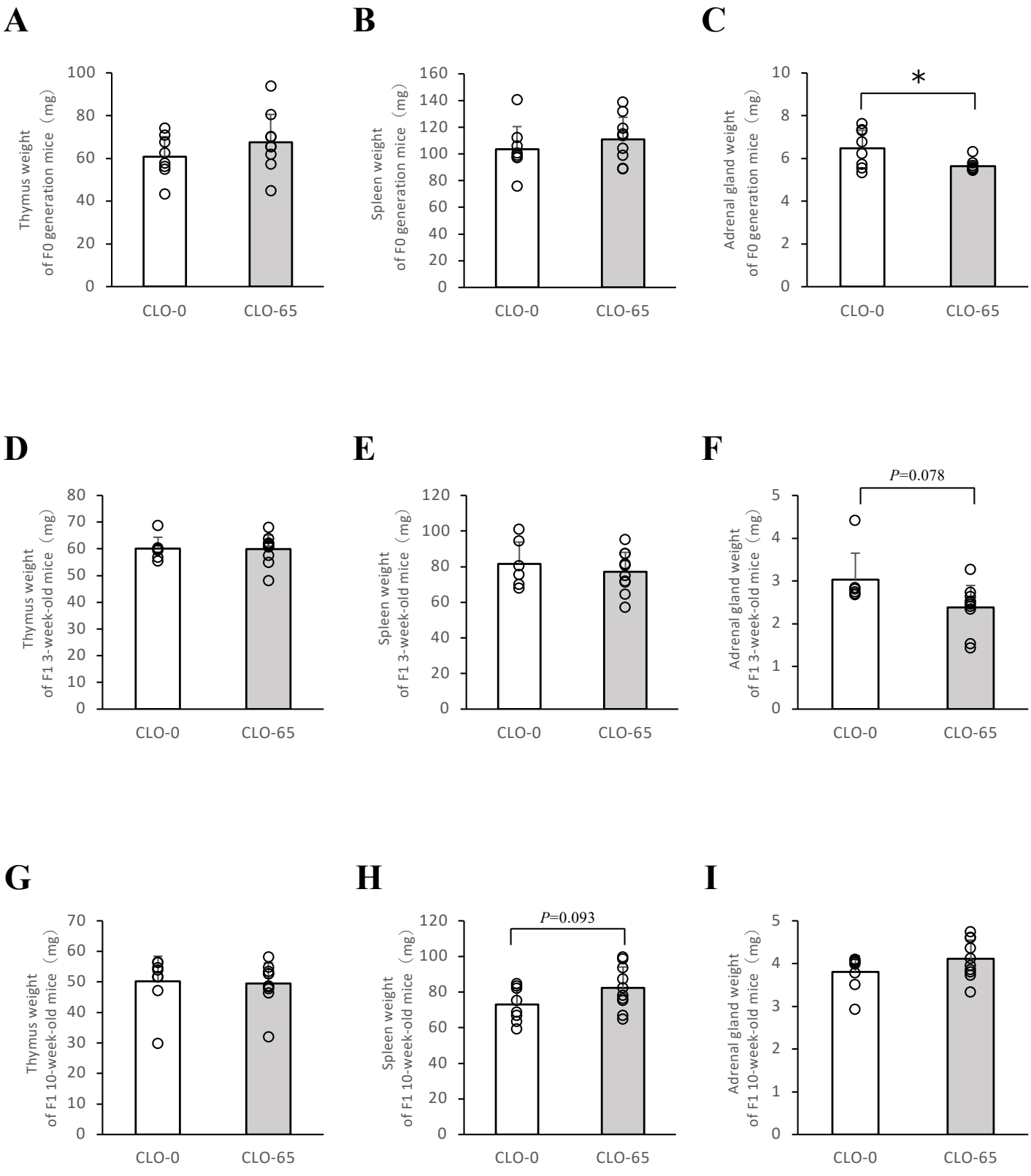
A
Thymus weight of F0 generation mice（mg）
100
80
60
40
20
0
CLO-0
CLO-65
B
Spleen weight of F0 generation mice（mg）
160
140
120
100
80
60
40
20
0
CLO-0
CLO-65
C
Adrenal gland weight of F0 generation mice（mg）
10
8
6
4
2
0
*
CLO-0
CLO-65
D
Thymus weight of F1 3-week-old mice（mg）
80
70
60
50
40
30
20
10
0
CLO-0
CLO-65
E
Spleen weight of F1 3-week-old mice（mg）
120
100
80
60
40
20
0
CLO-0
CLO-65
F
Adrenal gland weight of F1 3-week-old mice（mg）
P=0.078
5
4
3
2
1
0
CLO-0
CLO-65
G
Thymus weight of F1 10-week-old mice（mg）
70
60
50
40
30
20
10
0
CLO-0
CLO-65
H
Spleen weight of F1 10-week-old mice（mg）
P=0.093
120
100
80
60
40
20
0
CLO-0
CLO-65
I
Adrenal gland weight of F1 10-week-old mice（mg）
5
4
3
2
1
0
CLO-0
CLO-65

Fig. 2

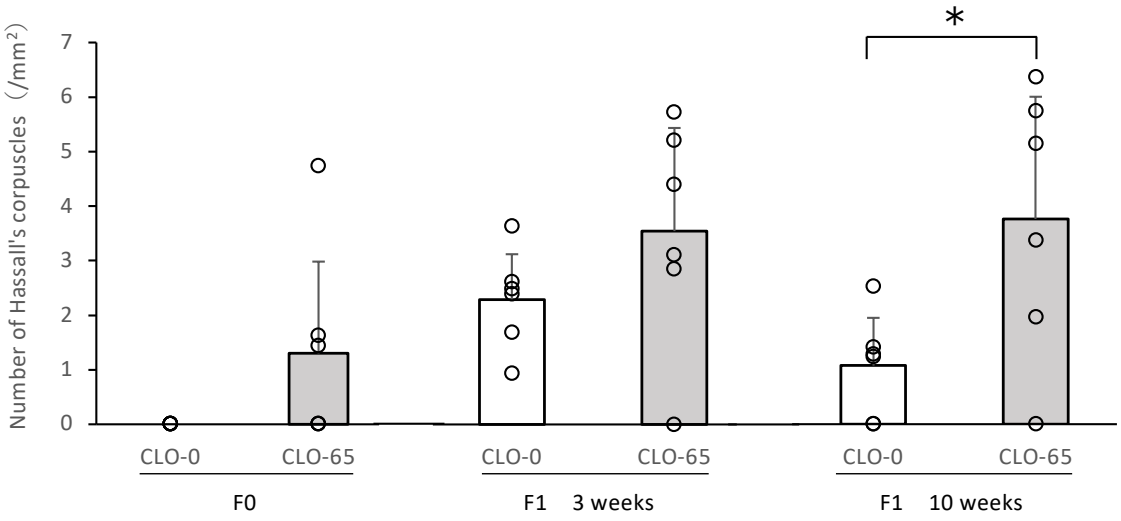
Number of Hassall's corpuscles (/mm²)
7
6
5
4
3
2
1
0
*
CLO-0
CLO-65
CLO-0
CLO-65
CLO-0
CLO-65
F0
F1 3 weeks
F1 10 weeks

Fig. 3

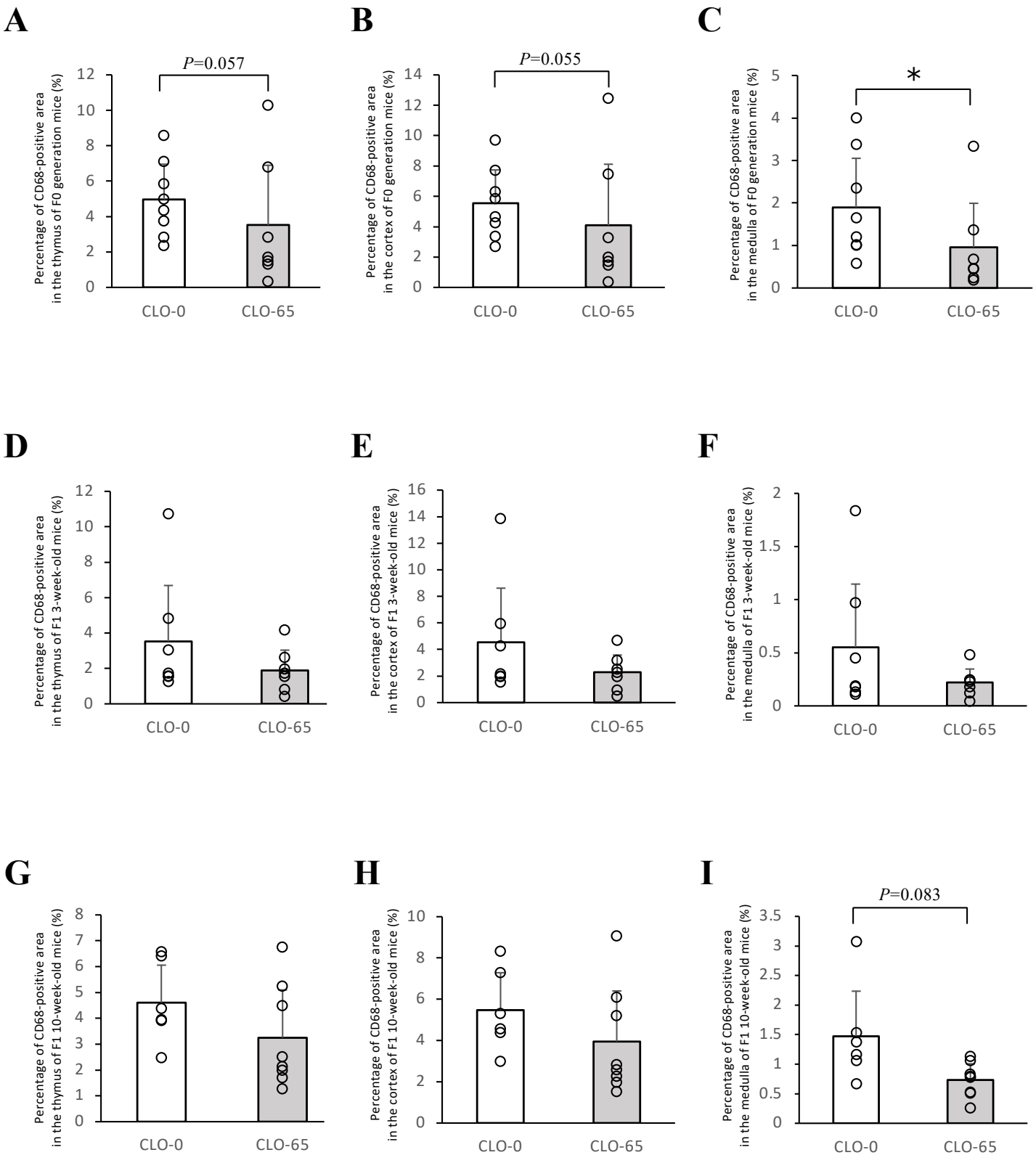
A
B
C
D
E
F
G
H
I
P=0.057
P=0.055
*
P=0.083
Percentage of CD68-positive area in the thymus of F0 generation mice (%)
Percentage of CD68-positive area in the cortex of F0 generation mice (%)
Percentage of CD68-positive area in the medulla of F0 generation mice (%)
Percentage of CD68-positive area in the thymus of F1 3-week-old mice (%)
Percentage of CD68-positive area in the cortex of F1 3-week-old mice (%)
Percentage of CD68-positive area in the medulla of F1 3-week-old mice (%)
Percentage of CD68-positive area in the thymus of F1 10-week-old mice (%)
Percentage of CD68-positive area in the cortex of F1 10-week-old mice (%)
Percentage of CD68-positive area in the medulla of F1 10-week-old mice (%)
CLO-0
CLO-65

Fig. 4

A

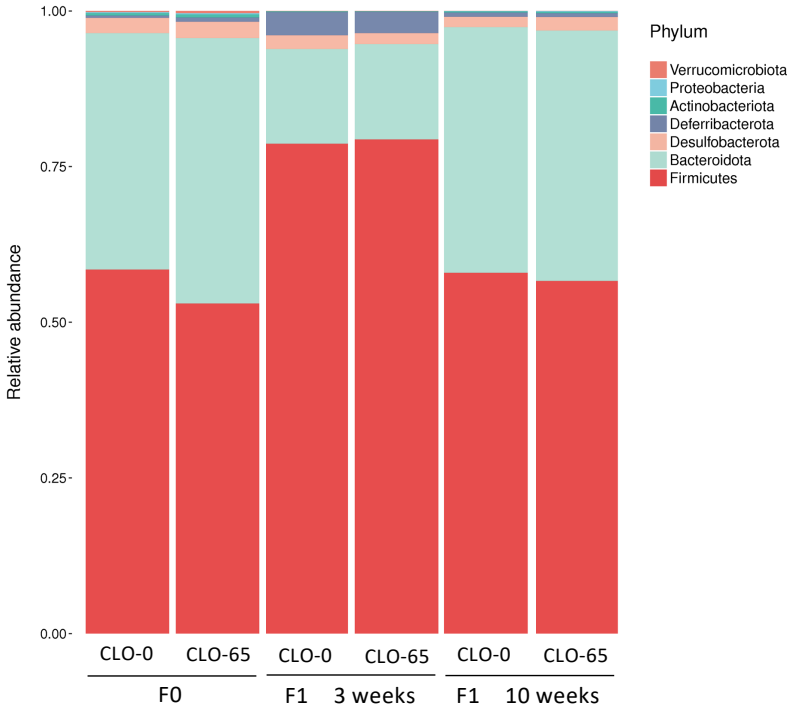
1.00
0.75
0.50
0.25
0.00
Relative abundance
Phylum
Verrucomicrobiota
Proteobacteria
Actinobacteriota
Deferribacterota
Desulfobacterota
Bacteroidota
Firmicutes
CLO-0
CLO-65
CLO-0
CLO-65
CLO-0
CLO-65
F0
F1
3 weeks
F1
10 weeks

B

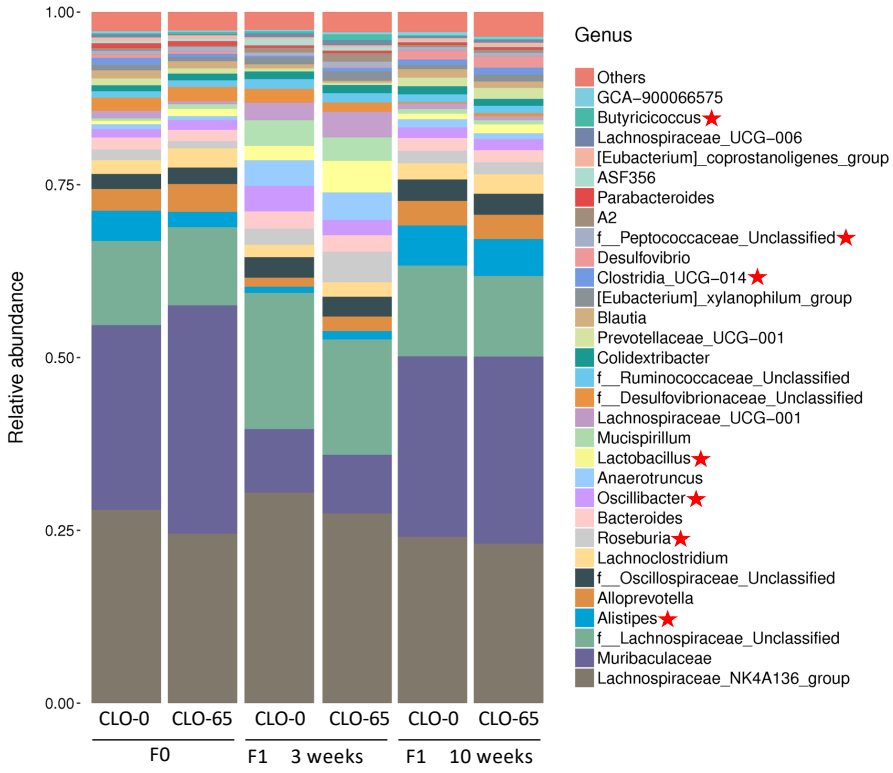
1.00
0.75
0.50
0.25
0.00
Relative abundance
Genus
Others
GCA–900066575
Butyricicoccus★
Lachnospiraceae_UCG–006
[Eubacterium]_coprostanoligenes_group
ASF356
Parabacteroides
A2
f__Peptococcaceae_Unclassified★
Desulfovibrio
Clostridia_UCG–014★
[Eubacterium]_xylanophilum_group
Blautia
Prevotellaceae_UCG–001
Colidextribacter
f__Ruminococcaceae_Unclassified
f__Desulfovibrionaceae_Unclassified
Lachnospiraceae_UCG–001
Mucispirillum
Lactobacillus★
Anaerotruncus
Oscillibacter★
Bacteroides
Roseburia★
Lachnoclostridium
f__Oscillospiraceae_Unclassified
Alloprevotella
Alistipes★
f__Lachnospiraceae_Unclassified
Muribaculaceae
Lachnospiraceae_NK4A136_group
CLO-0
CLO-65
CLO-0
CLO-65
CLO-0
CLO-65
F0
F1
3 weeks
F1
10 weeks

Fig. 5

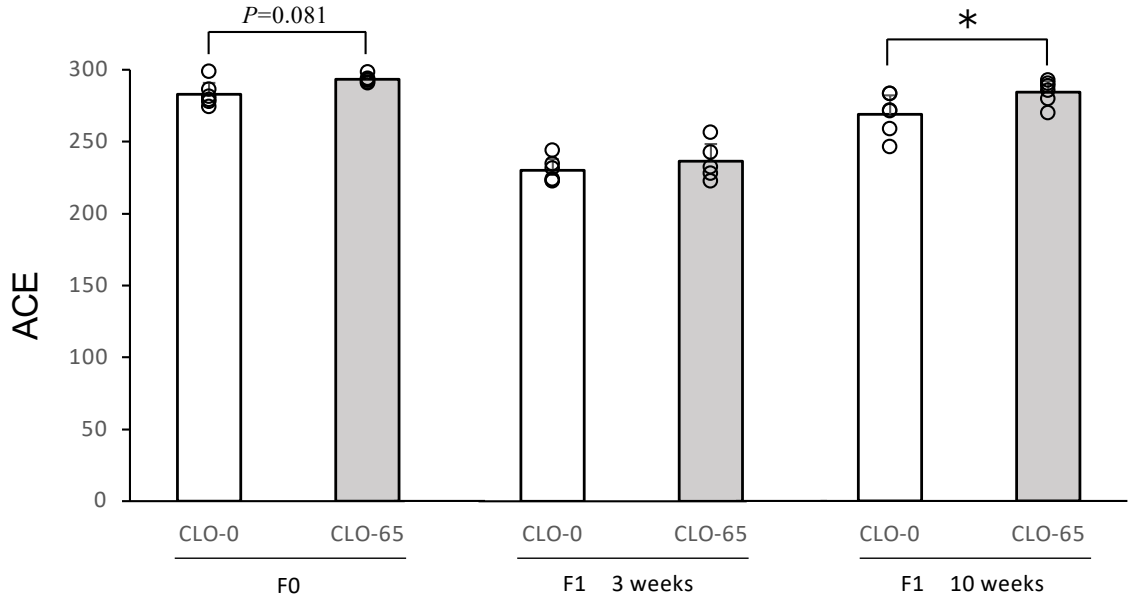
P=0.081
*
ACE
300
250
200
150
100
50
0
CLO-0
CLO-65
CLO-0
CLO-65
CLO-0
CLO-65
F0
F1 3 weeks
F1 10 weeks

Table 1. Body weight of F1 generation mice

	3-week-old		10-week-old	
	CLO-0	**CLO-65**	**CLO-0**	**CLO-65**
Body weight (g)	8.78 ± 0.81	8.83 ± 0.71	25.13 ± 0.83	25.88 ± 1.74

Mean ± SD (n = 8–25 in each)

Table 2. Genus-level microbiota showing significant changes or significant tendencies

Microbiota (genus)	Increase/Decrease	*P*-value (vs. CLO-0)	Characteristic
Alistipes	Decrease (F0 generation)	0.039	Involved in butyrate production and inversely correlated with intestinal inflammation [7].
Roseburia	Increase (F1 3-week-old)	0.036	Butyric acid-producing bacterium that also produces formic acid and lactic acid [10].
Oscillibacter	Decrease (F1 3-week-old)	0.028	May exacerbate DSS-induced colitis [30]. Negative correlation with the abundance of *lactobacilli* [56].
Lactobacillus	Increase (F1 3-week-old)	0.003	Ferments carbohydrates to produce lactic acid [5]. Depressed patients show a decreasing trend in relative abundance [1].
Clostridia_UCG-014	Decrease (F0 generation)	0.025	Positive correlation with IL-10 levels and negative correlation with the severity of colitis in a mouse model of *Bacillus cereus*-induced colitis [42].
f__Peptococcaceae_Unclassified	Increase (F1 3-week-old)	0.001	Decreased in patients with SLE, an autoimmune disease [3]. A mercury-methylating bacterium of the genus *Clostridium* [15]. It is involved in serine metabolism [20].
Butyricicoccus	Increase (F1 3-week-old)	0.018	A type of butyrate-producing bacteria [6].

Table 3. ANOSIM, a statistical indicator

Factor	*R*-value	*P*-value
F0 CLO-0 vs F0 CLO-65	0.056	0.274
F1 3-week-old CLO-0 vs F1 3-week-old CLO-65	0.263	0.055
F1 10-week-old CLO-0 vs F1 10-week-old CLO-65	-0.026	0.499

n = 6 in each

Fig. S1

A

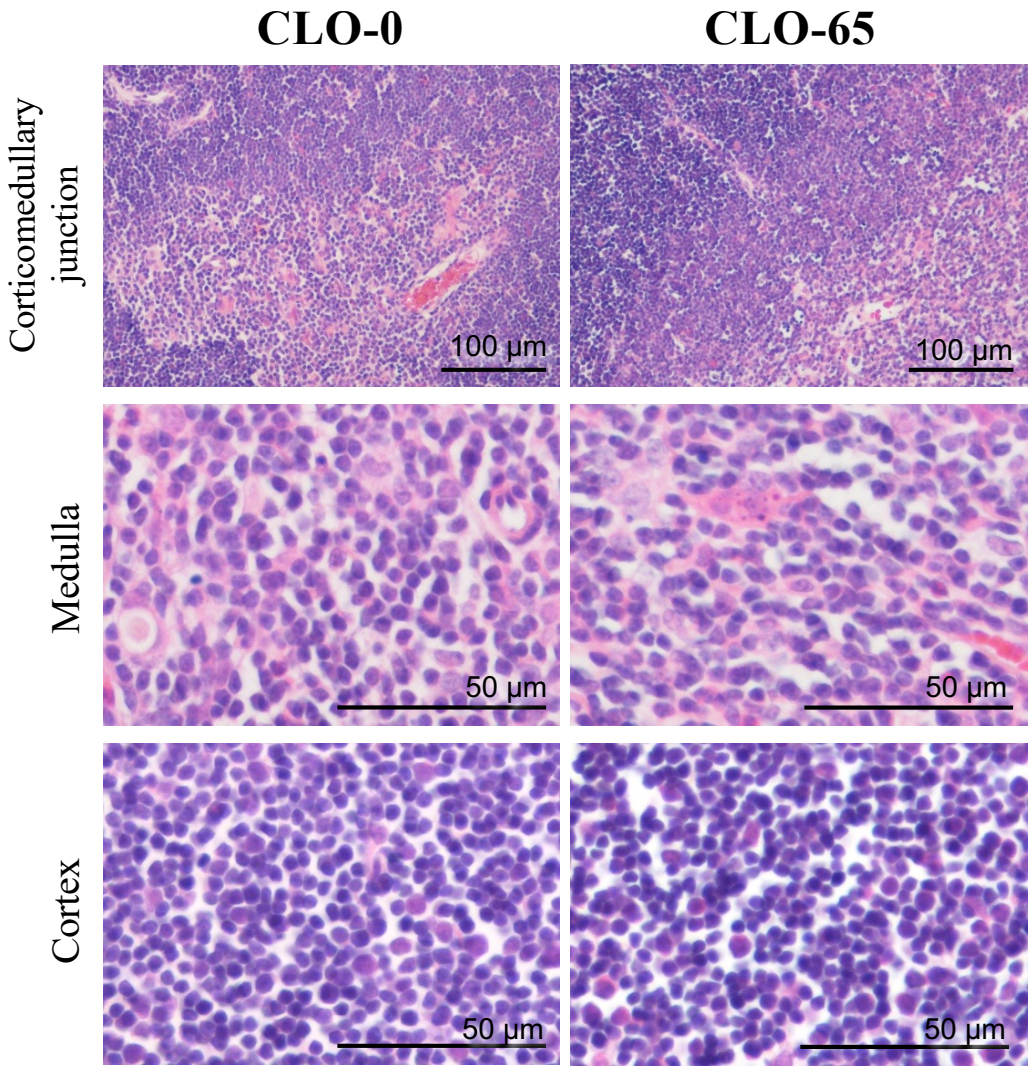
CLO-0
CLO-65
Corticomedullary junction
Medulla
Cortex
100 μm
100 μm
50 μm
50 μm
50 μm
50 μm

Fig. S1

B

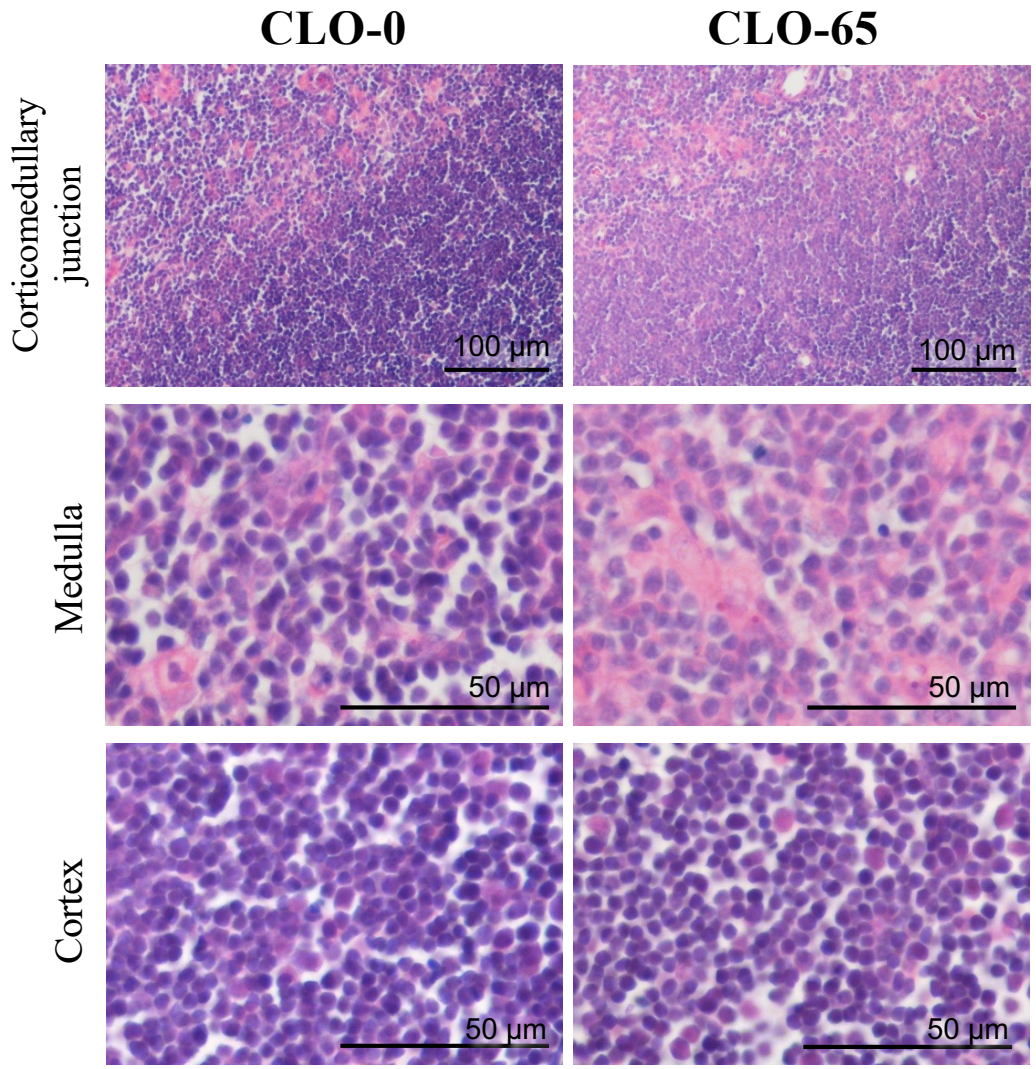
CLO-0
CLO-65
Corticomedullary junction
Medulla
Cortex
100 μm
100 μm
50 μm
50 μm
50 μm
50 μm

Fig. S1

C

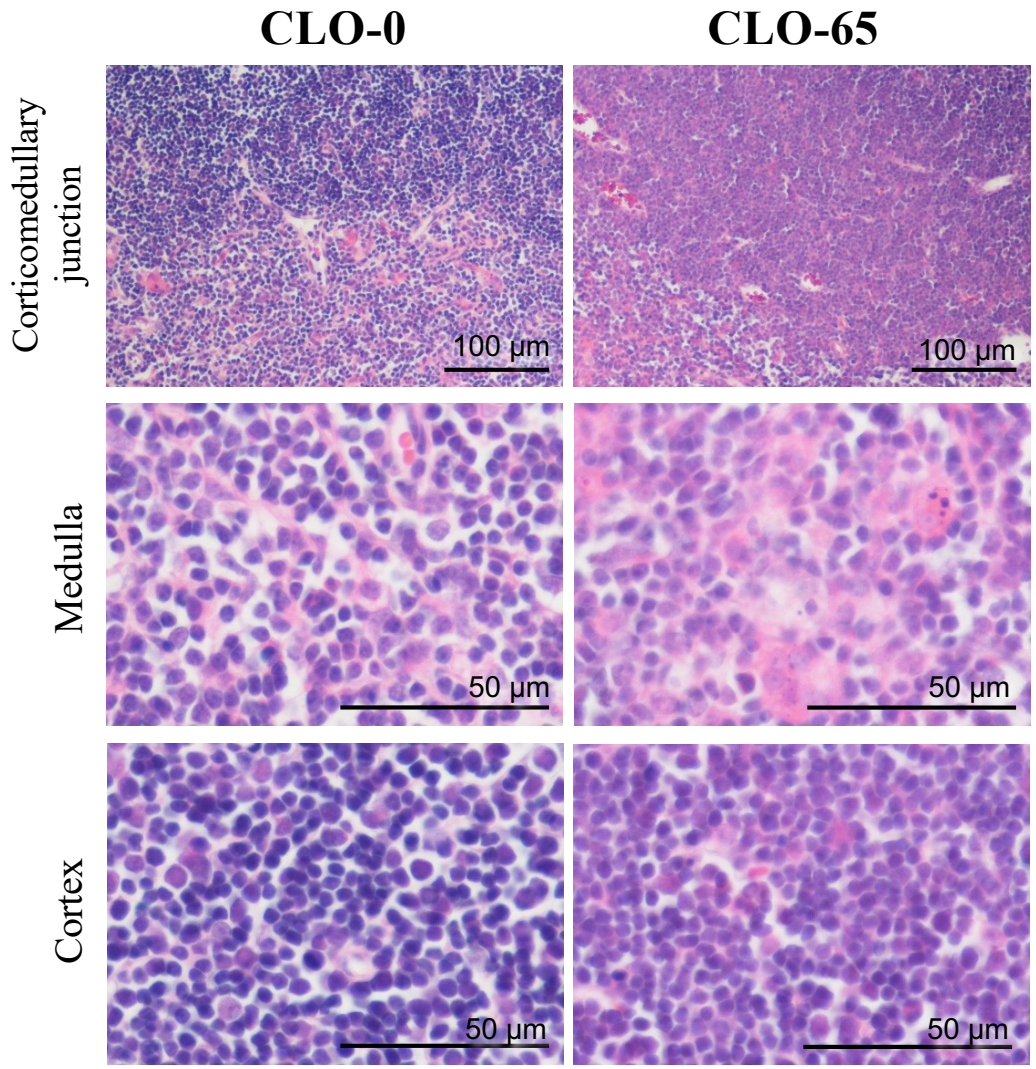
CLO-0
CLO-65
Corticomedullary junction
Medulla
Cortex
100 μm
100 μm
50 μm
50 μm
50 μm
50 μm

Fig. S2

A

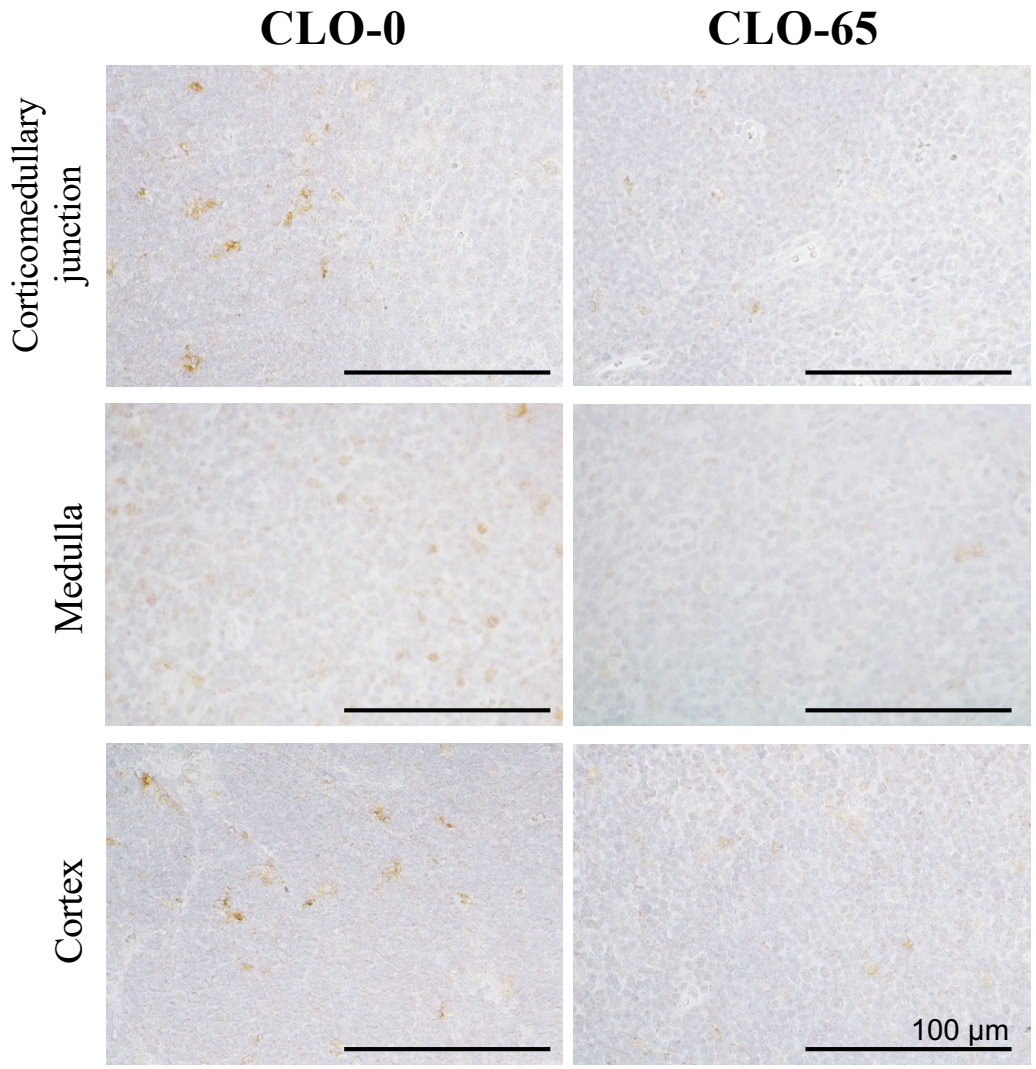
CLO-0
CLO-65
Corticomedullary junction
Medulla
Cortex
100 μm

Fig. S2

B

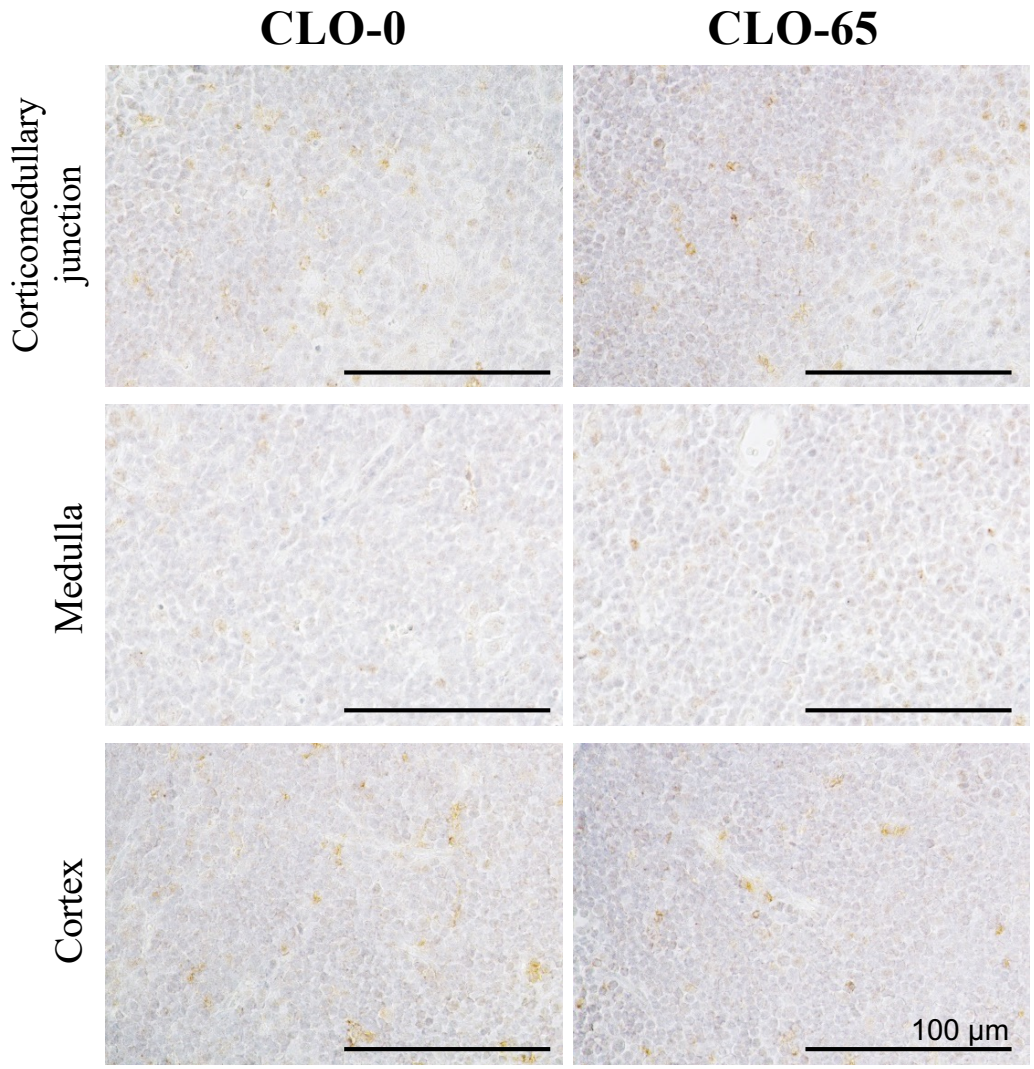
CLO-0
CLO-65
Corticomedullary junction
Medulla
Cortex
100 μm

Fig. S2

C

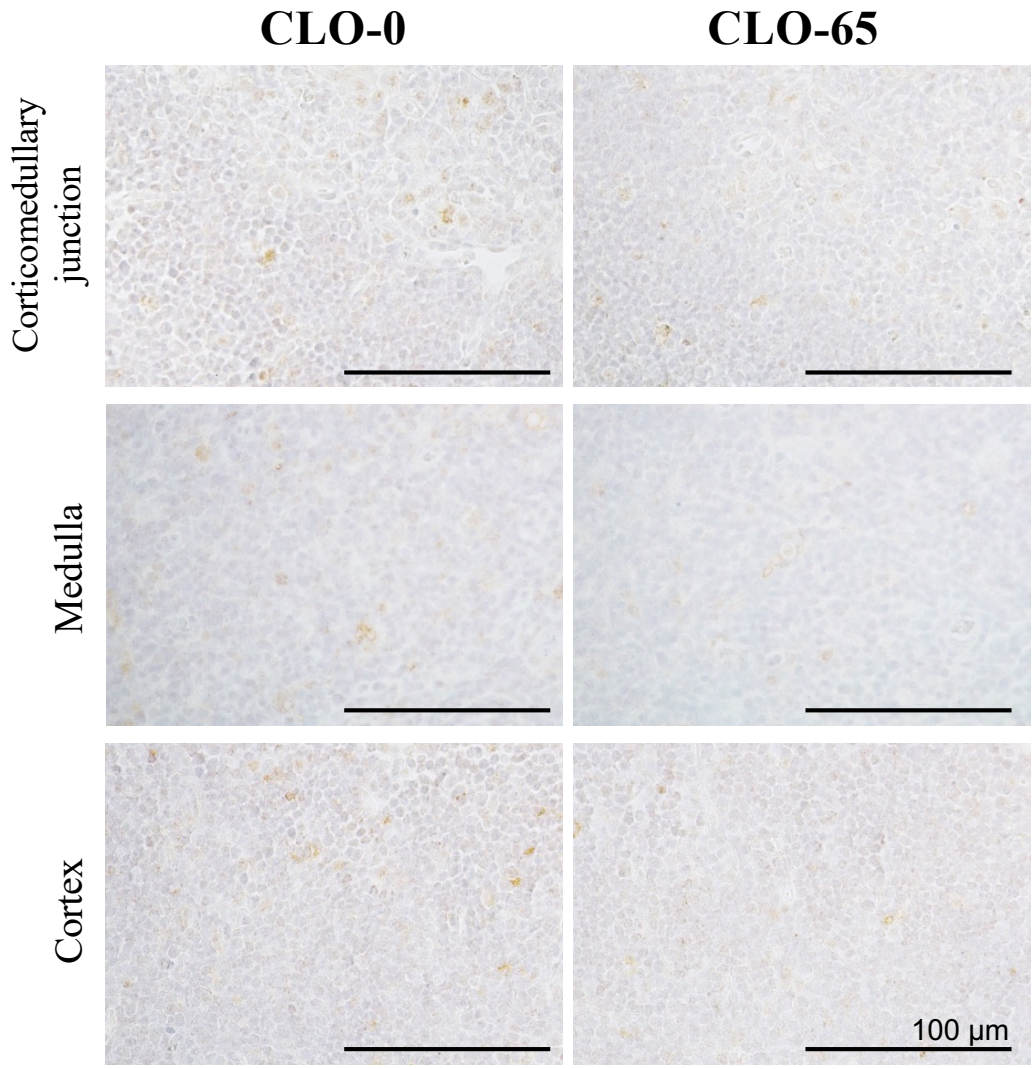
CLO-0
CLO-65
Corticomedullary junction
Medulla
Cortex
100 μm

Fig. S3

A

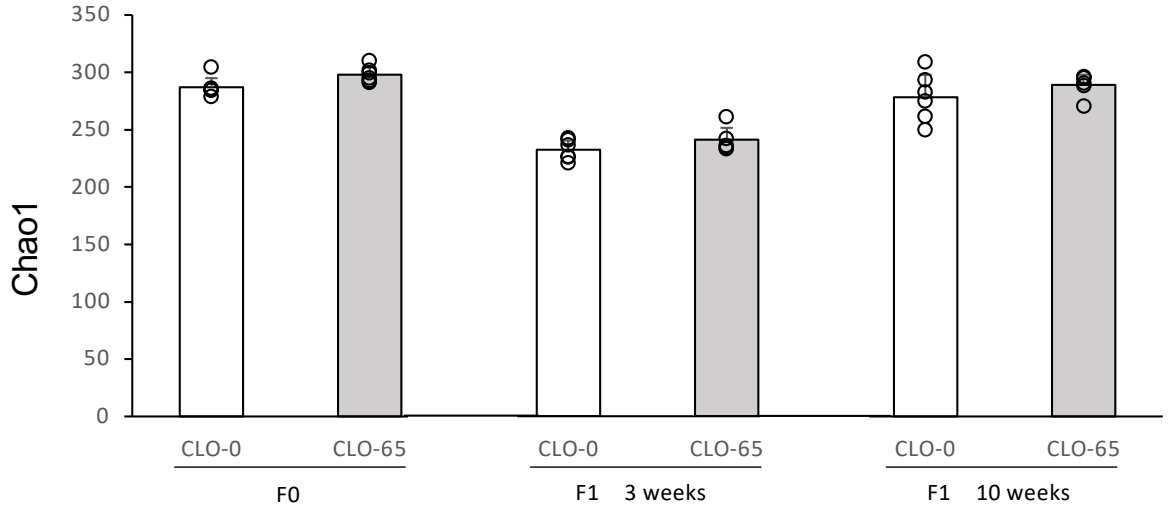
Chao1
350
300
250
200
150
100
50
0
CLO-0
CLO-65
CLO-0
CLO-65
CLO-0
CLO-65
F0
F1 3 weeks
F1 10 weeks

B

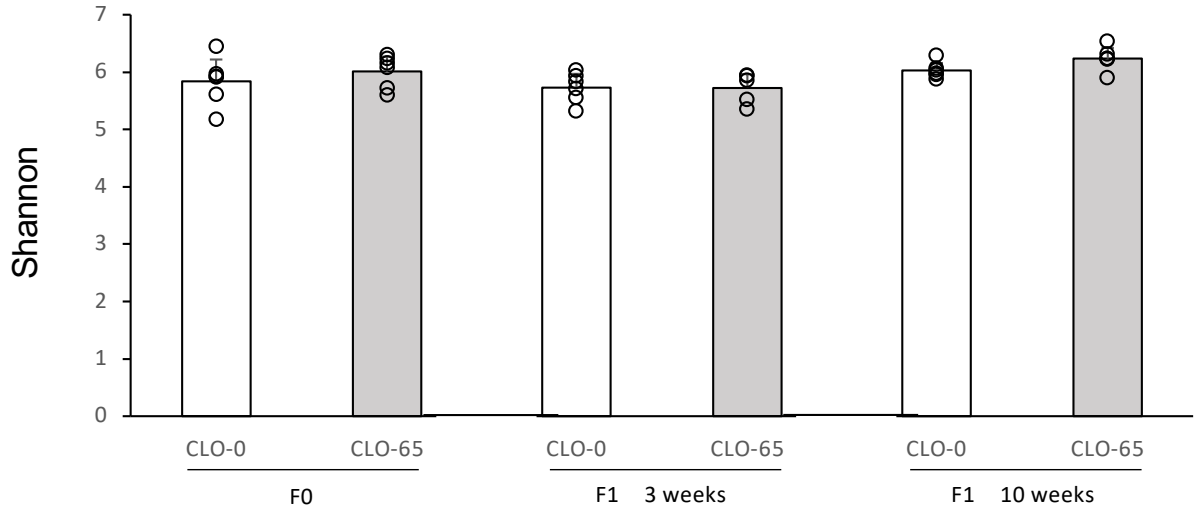
Shannon
7
6
5
4
3
2
1
0
CLO-0
CLO-65
CLO-0
CLO-65
CLO-0
CLO-65
F0
F1 3 weeks
F1 10 weeks

C

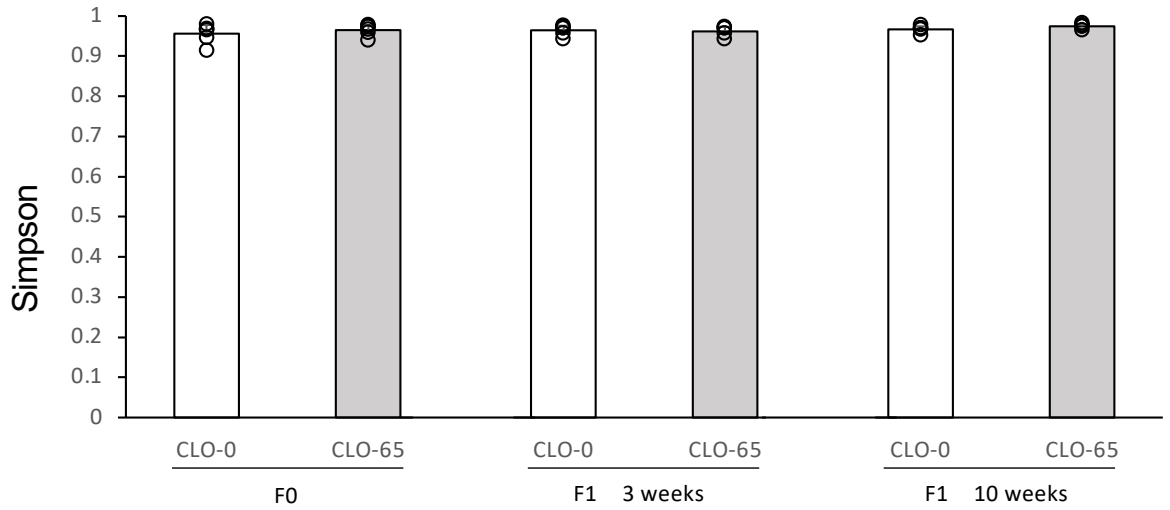
Simpson
1
0.9
0.8
0.7
0.6
0.5
0.4
0.3
0.2
0.1
0
CLO-0
CLO-65
CLO-0
CLO-65
CLO-0
CLO-65
F0
F1 3 weeks
F1 10 weeks

Fig. S4

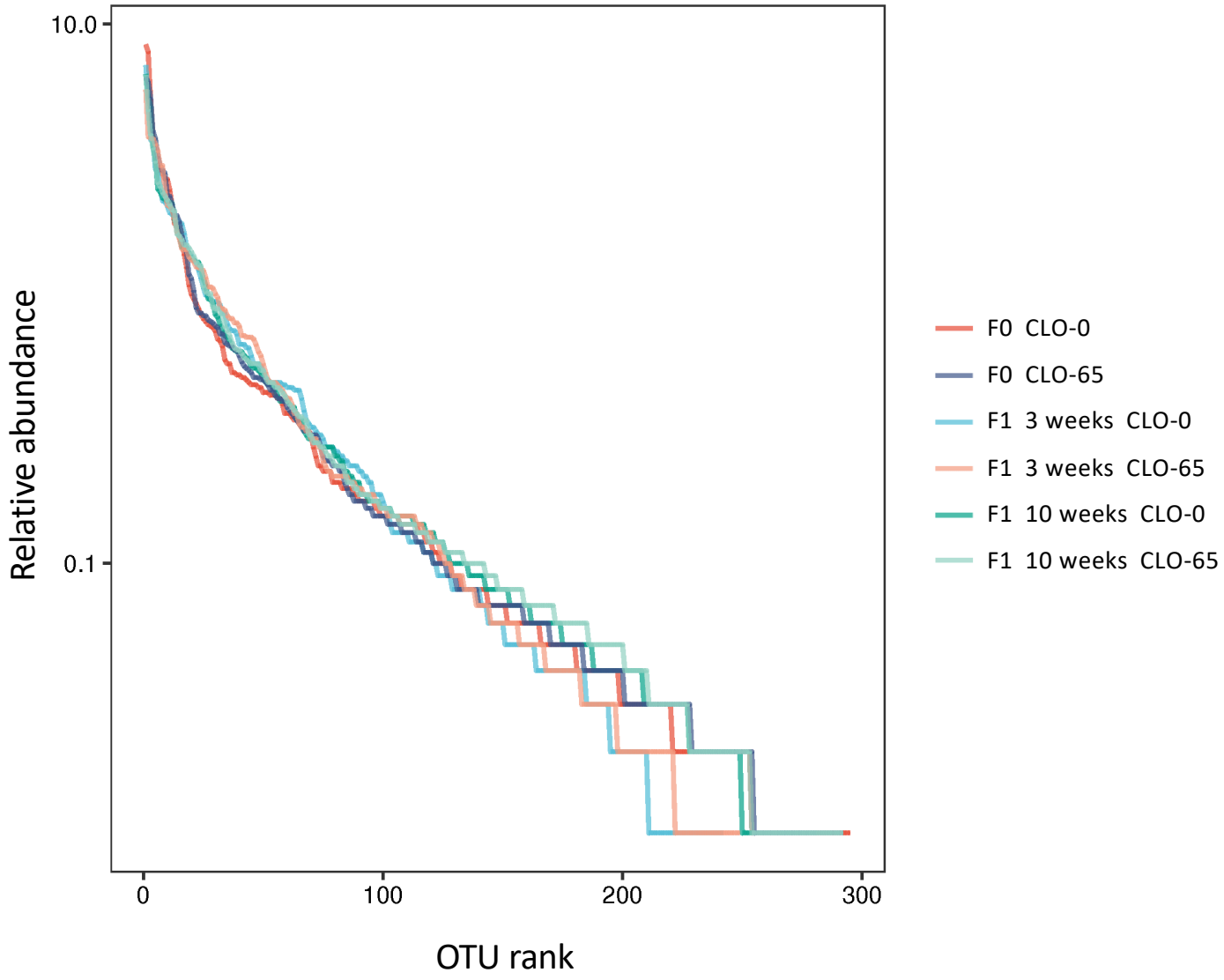
10.0
0.1
Relative abundance
0
100
200
300
OTU rank
F0 CLO-0
F0 CLO-65
F1 3 weeks CLO-0
F1 3 weeks CLO-65
F1 10 weeks CLO-0
F1 10 weeks CLO-65

Fig. S5

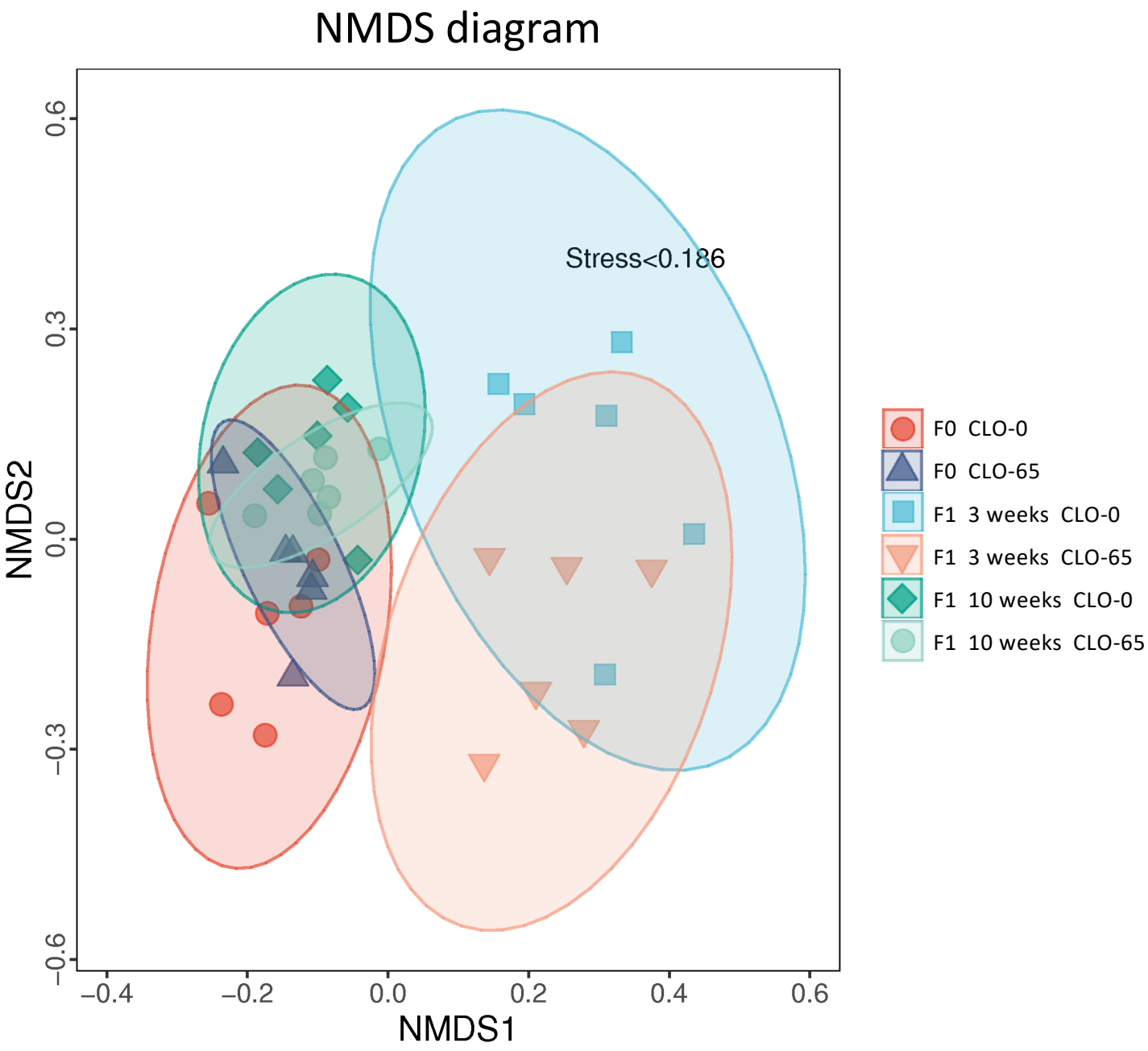
NMDS diagram
Stress<0.186
NMDS1
NMDS2
0.6
0.3
0.0
−0.3
−0.6
−0.4
−0.2
0.0
0.2
0.4
0.6
F0 CLO-0
F0 CLO-65
F1 3 weeks CLO-0
F1 3 weeks CLO-65
F1 10 weeks CLO-0
F1 10 weeks CLO-65